

Material Defects Identification in Metal Ceramic Fixed Partial Dentures by En-Face Polarization Sensitive Optical Coherence Tomography

C. Sinescu, M. Negrutiu, R. Negru, M. Romînu, A.G. Podoleanu

Abstract—The fixed partial dentures are mainly used in the frontal part of the dental arch because of their great esthetics. There are several factors that are associated with the stress state created in ceramic restorations, including: thickness of ceramic layers, mechanical properties of the materials, elastic modulus of the supporting substrate material, direction, magnitude and frequency of applied load, size and location of occlusal contact areas, residual stresses induced by processing or pores, restoration-cement interfacial defects and environmental defects. The purpose of this study is to evaluate the capability of Polarization Sensitive Optical Coherence Tomography (PSOCT) in detection and analysis of possible material defects in metal-ceramic and integral ceramic fixed partial dentures. As a conclusion, it is important to have a non invasive method to investigate fixed partial prostheses before their insertion in the oral cavity in order to satisfy the high stress requirements and the esthetic function.

Keywords—Ceramic Fixed Partial Dentures, Material Defects, Polarization Sensitive Optical Coherence Tomography, Numerical Simulation

I. INTRODUCTION

The longevity of dental restorations is an important health concern. Longitudinal studies are appropriate to give an exact insight into the longevity of restorations [Leempoel et al.1989]. A prosthetic restorative system can be considered successful if it demonstrates a survival rate of 95% after 5 years and 85% after 10 years [Probster 1996]. The long-term success of fixed partial dentures can be affected by factors related to the patient, processing or the operator [Kerschbaum 1999]. Patient-related factors include: risk of caries (high

numbers of cariogenic bacteria, low local fluoride intake, high sugar intake, low salivary rate), risk of periodontitis (poor oral hygiene, smoking, genetic factors), bruxism, participation in contact sports.

Processing- and operator-related factors include: poor diagnosis (poor assessment of caries and periodontitis, short crown length), inadequate preoperative treatment (lack of lowering of existing risk, tooth cleaning, instruction in oral hygiene), unsuitable design of the restoration for the given situation (e.g., does not meet Ante's law, bruxism), inappropriate preparation (e.g., non-retentive in conjunction with conventional cementation, minimal occlusal reduction), poor impression technique, esthetics that are not tailored to the patient, sloppy fabrication of the bridge in the dental laboratory (overhangs, nonphysiological design of the interdental embrasure), inappropriate placement of a bridge (inadequate moisture control, incorrect processing of bridge insertion) and inadequate recall schedule [Marianna Grigoriadou, 2006]. Metal-ceramic fixed partial dentures are considered a standard treatment modality in dental practice. Therefore, their survival rate should be used as criterion for new all-ceramic systems. In a long-term clinical study, 102 patients received 108 fixed partial dentures made of cast gold and heatcured acrylic veneering. The restorations were made by the senior students of the Dental Faculty at the University of Oslo. The survival rate was 96%, 88% and 68% after observation periods of 5, 10 and 15 years, respectively [Valderhaug 1991]. In a meta-analysis, the outcome of 4118 fixed partial dentures showed that the restorations had a survival rate of 74% after 15 years [Creugers et al. 1994]. Leempoel (1995) analyzed the survival rate of 1674 fixed partial dentures placed in 40 Dutch general practices and the influence of several factors on prosthesis lifetime, and reported a survival rate of 87% after an observation period of 12 years. In another meta-analysis, less than 15% of the fixed partial dentures were removed or needed to be replaced at 10 years, whereas only one third were removed or needed to be replaced at 15 years [Scurria 1998]. Walton (2002) examined the survival rate of 515 metal-ceramic fixed partial dentures placed by one operator in a specialized prosthodontic practice, and reported that tooth-supported fixed partial dentures have an estimated survival rate of 96%, 87% and 85% at 5, 10 and

Cosmin Sinescu is with the University of Medicine and Pharmacy Victor Babes from Timisoara, Romania, Faculty of Dentistry, Dental Materials and Dental Technologies Department (corresponding author to provide phone: +40722280132; e-mail: minosinescu@yahoo.com).

Meda Negrutiu. is with the University of Medicine and Pharmacy Victor Babes from Timisoara, Romania, Faculty of Dentistry, Dental Materials and Dental Technologies Department (e-mail: meda_negrutiu@yahoo.com).

Radu Negru is with the University of Politehnica from Timisoara, Romania (e-mail:blackradu@yahoo.com).

Mihai Romînu is with the University of Medicine and Pharmacy Victor Babes from Timisoara, Romania, Faculty of Dentistry, Dental Materials and Dental Technologies Department (e-mail: mrominu@hotmail.com).

Adrian Gh. Podoleanu is with the Applied Optics Group, University of Kent, Canterbury, UK (e-mail: A.G.H.Podoleanu@kent.ac.uk).

15 years, respectively [Marianna Grigoriadou, 2006]. B. Taskonak, J.J. Mecholsky, Jr. and K.J. Anusavice investigated the fracture surface analysis of clinically failed fixed partial dentures (2006). The objective of this study was to determine the site of crack initiation and the causes of fracture of clinically failed ceramic fixed partial dentures. Six Empress 2® lithia-disilicate ($\text{Li}_2\text{O}\cdot 2\text{SiO}_2$)-based veneered bridges and 7 experimental lithia-disilicate-based non-veneered ceramic bridges were retrieved and analyzed. Fractography and fracture mechanics methods were used to estimate the stresses at failure in 6 bridges (50%) whose fracture initiated from the occlusal surface of the connectors. Fracture of 1 non-veneered bridge (8%) initiated within the gingival surface of the connector. Three veneered bridges fractured within the veneer layers. Failure stresses of the all-core fixed partial dentures ranged from 107 to 161 MPa. Failure stresses of the veneered fixed partial dentures ranged from 19 to 68 MPa [1, 2]. Making metal-ceramic or integral fixed partial dentures can lead to aeric inclusions in the ceramic layers that could initiate materials defects and lines of fracture in the aesthetic parts of the dentures [12]. The common investigations methods of fixed partial dentures imply sectioning and metallographic microscopic analysis (Fig.1.). These methods could lead to damage of the small dimension material defects. Also these methods are limited to the dimensions of the cutting devices [1, 2].

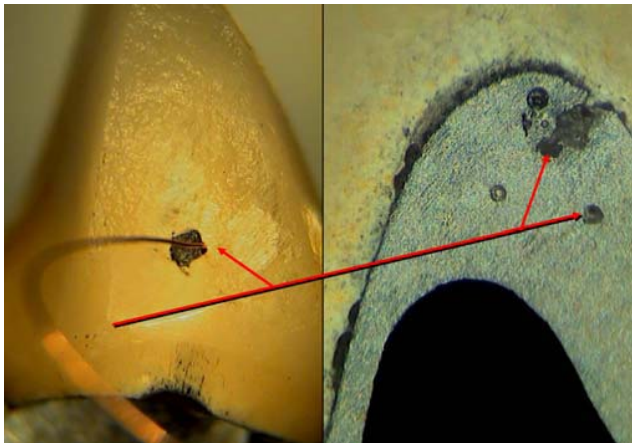


Fig. 1. The common investigations methods of fixed partial dentures imply sectioning and metallographic microscopic analysis.

Noninvasive research methods are very useful in characterizing the infrastructure of the fixed partial bridges, due to the possibility of using the support after the evaluation in order to make a good and much more resistant dental bridge. One of these characterizing methods is the penetrating liquids method. This method allows discovering the materials defects of the infrastructure, but only the ones that are connected to the surface. The method is based on the flowing property of the liquids. In order to discover the defects in the dental bridge infrastructure, a penetrating liquid, containing three sprays chit is used. The first spray is used for cleaning the surface of the fixed partial denture. The second spray contains the penetration liquid. This one is going to fill all the material

imperfections of the bridge. The last spray contains the revelator liquid and this one reveals the areas where the defects are. In the first faze, the bridge is cleaned by using the first spray. The reason for this action is that the little particles of dust can obdurate the access of the liquid in the defect areas. After this first faze, the bridge needs to be dried in order to use the second spray. Using the second spray is the next step in this procedure. Between the second and the third spray, a break of ten minutes must be made to permit the penetrating liquid to fill all the defects of the structure. After this break, the excess of the penetrating liquid is cleaned out. Afterwards, the revelator liquid is used to point out the areas with material discontinuities (Fig. 2).



Fig. 2. The penetrating liquid method is used to point out the areas with material discontinuities.

The penetrating liquids method is a nondestructive method used for evaluating the continuity of the materials from which the dental works are made. By using this method, every defect zone that has any connection to the surface of the bridge can be revealed. The cost of this method is very low and the results are obtained rapidly and accurate. However, for the defects that are included in the core of the fixed partial dentures, this method has no applications [1, 10, 12]. For the fixed partial dentures micro leakage investigations it is possible to use the method of laser micro spectral analysis [1]. This method was first introduced in 1962, and was used specially to investigate the surface of metals. The method was reconsidered these years, when is also known as the method of spectroscopy by laser induced plasma. This method also requires low costs, compared with other point-like methods such as X-ray fluorescence spectroscopy or neutron activation method. The laser micro spectral analysis device LMA-10 (Carl Zeiss, Jena) was used equipped with a diffraction spectrometer PGS-2 (Carl Zeiss, Jena). The output energy of the laser is 0.5-1.2 Joule/pulse, $\lambda=1060$ nm. The LMA-10 system has mirror lens 40x, used to visualize the explored surface, which can be interchanged with 10 X lens, used to focus the laser pulse. Different fixed partial dentures (metal-polymeric) were used in order to determine the micro leakage between the metal infrastructure and the polymer part. The fixed partial dentures were fixed on the microscope table in a

piece of wax, so that the section was positioned horizontally. The distribution of chemical elements infiltrations was investigated by making a series of craters, and establishing the spectra of the vapours emitted from the craters. The displacement along these directions and the measurement of position of the craters was possible due to the micro-displacement system of the microscope table, and to the reticular scale of the mirror microscope lens (Fig. 3). This method is a quantitative but an invasive one and affect irreversible the investigated samples [10, 12].



Fig.3. The method of laser micro spectral analysis is a method of punctual method of analysis, which allows to investigate small quantity of material, around 0.1 μg .

The purpose of this study is to analyze the existence of possible fractures in several metal ceramic fixed partial dentures using a non invasive method.

II. MATERIALS AND METHODS

A. Different Scanning Procedures

To obtain 3D information about an object under investigation, any imaging system is equipped with three scanning means, one to scan the object in depth and two others to scan the object transversally. Depending on the order these scanners are operated and on the scanning direction associated with the line displayed in the raster of the final image delivered, different possibilities exist.

B. Longitudinal OCT (A-scan based B-scan)

B-scan images, analogous to ultrasound B-scan are generated by collecting many reflectivity profiles in depth (A-scans) for different and adjacent transverse positions. The transverse scanner (operating along X or Y) advances at a slower pace to build a B-scan image. The majority of reports in literature refer to this method of operation. In longitudinal OCT, the axial scanner is the fastest and its movement is synchronous with displaying the pixels along the line in the raster, while the lateral scanning determines the frame rate.

C. En-face OCT (T-scan based B-scan)

In this case, the transverse scanner determines the fast lines in the image. We call each such image line a T-scan. This can be produced by controlling either the transverse scanner along the X-coordinate, or along the Y-coordinate with the other two scanners fixed. This procedure has a net advantage in comparison with the A-scan based B-scan procedure as it allows production of OCT transverse (or 2D *en-face*) images for a fixed reference path, images called C-scans. In this way, the system can be easily switched from B to C-scan, a procedure incompatible with A-scan based OCT imaging.

D. C-scan

C-scans are made from many T-scans along either of X, Y, repeated for different values of the other transverse coordinate, Y, X respectively in the transverse plane. The repetition of T-scans along the other transverse coordinate is performed at a slower rate than that of the T-scans, which determines the frame rate. In this way, a complete raster is generated. Different transversal slices are collected for different depths Z, either by advancing the optical path difference in the OCT in steps after each complete transverse (XY) scan, or continuously at a much slower speed than the frame rate. The depth scanning is the slowest in this case.

E. The Experimental Configuration

Two *en-face* OCT systems have been used. Both use similar pigtailed super-luminescent diodes (SLD) emitting at 1300 nm and having spectral bandwidths of 65 nm which determine an OCT longitudinal resolution of around 17.3 microm in tissue. The first OCT system performs OCT only, in both C-scan and B-scan regimes, with low NA, allowing 1 cm lateral image size. The second system, equipped with a confocal channel at 970 nm, uses a high NA interface optics allowing 1 mm image size. The configuration of the second system, as shown in Fig. 2, uses two single mode directional couplers. Light from the SLD source is injected into the system via the directional coupler DC1 which splits the light towards the two arms of the interferometer, the probing and the reference arm respectively. The probing beam is reflected by the dichroic beam-splitter BS1 and then sent via the galvanometer scanners SX and SY to the sample. Two telescopes incorporated between these elements conveniently alter the diameter of the beam in order to match the aperture of different elements in the probing path and convey a probing beam of around 8 mm in diameter through the microscope objective MO's pupil plane. Hence, a lateral resolution of around 2 μm in the confocal channel could be achieved. A transversal resolution better than 5 microns is obtained in the OCT channel. Light back-scattered by the sample passes a second time through the object arm and is guided towards the single mode directional coupler DC2 via DC1 where it interferes with that coming from the reference arm. Both output fibers from DC2 are connected to two pin photo-detectors in a balanced photo-detection unit. A computer driven translation stage (TS) is used to construct B-scan images by stopping the frame scanner and moving TS along the optical axis of the reference beam [3, 8].

The scanning procedure is similar to that used in any confocal microscope, where the fast scanning is *en-face* (line rate) and the depth scanning is much slower (at the frame rate). The *en-face* scans provide an instant comparison to the familiar sight provided by direct view or by a conventional microscope. Features seen with the naked eye can easily be compared with features hidden in depth. Sequential and rapid switching between the *en-face* regime and the cross-section regime, specific for the *en-face* OCT systems, represents a significant advantage in the non-invasive imaging as images with different orientations can be obtained using the same system [7, 8].

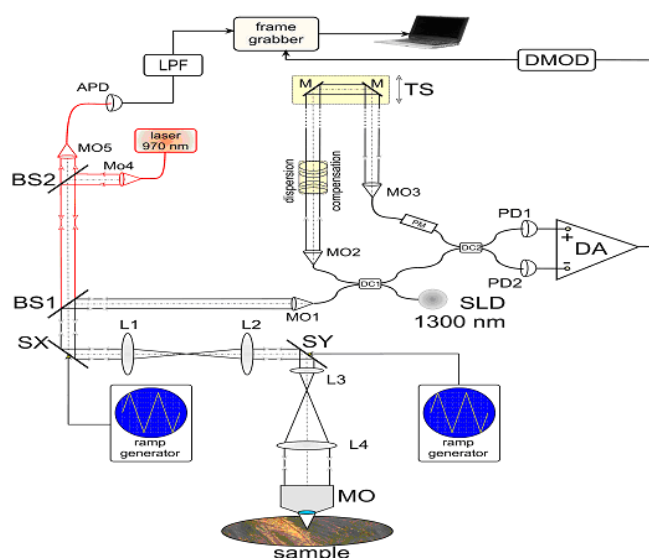


Fig. 2. – En-face OCT at 1300 nm/confocal at 970 nm system. SLD = superluminescent diode; SX, SY: X and Y scanners; IMG = index matching gel; APD: avalanche photodiode; L1, L2, L3, L4: lenses; MO1-5: microscope objectives; PD1, 2: pin photodetectors; BS1,2: beam splitters; LPF: low pass filter; PM: polarization.

As shown in Fig. 2, in the *en-face* regime, the frame grabber is controlled by signals from the generators driving the X-scanner and the Y-scanner. One galvo-scanner is driven with a ramp at 500 Hz and the other galvo-scanner with a ramp at 2 Hz. In this way, an *en-face* image, in the plane (x, y) is generated at constant depth. The next *en-face* image at a new depth is then generated by moving the translation stage in the reference arm of the interferometer and repeating the (x, y) scan. Ideally, the depth interval between successive frames should be much smaller than the system resolution in depth and the depth change applied only after the entire *en-face* image has been collected. However, in practice, to speed up the acquisition, the translation stage was moved continuously. Alternatively, a scanning delay line could be used, which can achieve faster depth scanning rates. In the images presented below, no other phase modulation was employed apart from that introduced by the X-galvanometer scanner. We demonstrated in a previous study the role played by the image size in balancing the effects of an external phase modulator and of the modulation produced by the transversal scanner. If

the image is sufficient large, then the distortions introduced by not using a phase modulator are insignificant.

The other system contains an OCT channel only, and the X and Y scanners are grouped spatially. Only one lens L of focal length 4 cm is used between the XY scanner head, allowing a larger lateral size image and a coarser transversal resolution in comparison with the second system, of only 15 microns. The X and Y scanners are similar and driven at the same line rate (500 Hz) and frame rate (2 Hz) as in the previous system. In the cross-section regime, the frame grabber is controlled by signals from the generator driving the X-scanner (or the Y-scanner) with a ramp at 500 Hz and the translation stage moving over the depth range required in 0.5 s. In this case, an OCT cross-section image is produced either in the plane (x, z) or (y, z) [3, 7, 8].

F. Metal Ceramics Fixed Partial Dentures

133 metal ceramics fixed partial dentures was investigated using Polarization Sensitive Optical Coherence Tomography as a non invasive method. 118 slices were used for each set of investigation. The distance between the slices was 20 microns. A 3D reconstruction was made for each investigation in order to evaluate the position and the magnitude of the ceramic defect.

G. Numerical Simulation Investigation

Numerical simulation investigations using finite elements method (F.E.M.) were developed in order to study the stress distribution in the fixed partial dentures in the masticator environment. The virtual models of the considerable fixed partial dentures were developed using manual design and scanners (mechanical and laser scanners). For all cases the obtained results pointed out the most tensioned zones for each dental construct which represented the targeted investigation zones for the PSOCT technique.

After the detection of the materials defects the numerical simulation method was used in order to estimate the effect of the masticatory forces on the fractures propagations in the ceramic materials. The numerical simulation was performed in FEM using COSMOS/M software package. The discretization of the structure was performed in an automatic mode using a triangular finite element (TRIANG, as a 3- to 6-node triangular, two-dimensional element for plane stress, plane strain, or ax symmetric structural and thermal models). In order to simulate the cracking of metal ceramic fixed partial dentures a fracture analysis code FRANC2D/L was used.

III. NUMERICAL SIMULATION RESULTS FOR PSOCT INVESTIGATIONS

The used apparatus for scanning is called MODELA and can scan through contact, step by step, the shape of a solid object. The sum of identified solid spots is mathematical processed and transformed into a 3D virtual image (Fig.3.). Before scanning, we have to attach the sensorial unite and the head for scanning. The sensor's force is a few tens grams, and can not scan objects which are modifying theirs shape at the sensor's touch. The error can be of maximum 0.5mm and it depends by the object's shape. The maximum scanned area is

150mm on OY direction, 100mm on OX and 60mm on OZ direction (maxim height). The soft used for this scanning is called Dr. PICZA and permit the partial shift of scanning steps.



Fig.3. The scanning system.

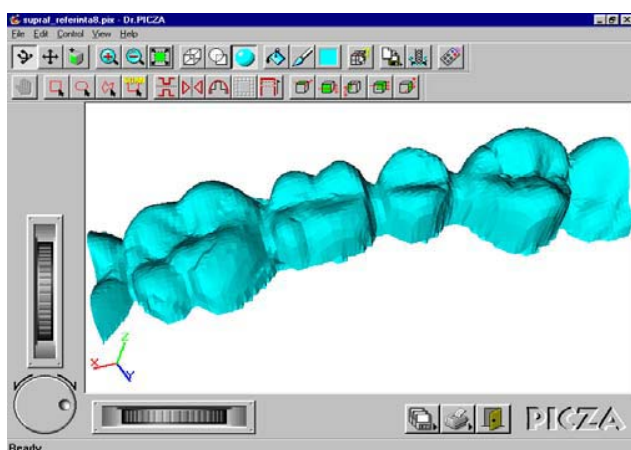


Fig.4. Aspects during the scanning process.

After making all measurements with special devices, the files are saved with *.igs extension (this document is recognized by all the 3D CAD systems). In the second stage, all the files are imported in programs for reconstruction- 3D shaping of CAD type as PROENGINEER igs. If the surface is continuous, the "Wire-frame" representation is in just one color. All the discontinuous surfaces are marked with yellow. For 3D shaping it is necessary a continuous surface. The import of *.igs file in PROENGINEERING maintains the three plans which define the system's coordinates and the taken measurements. The surface in PROENGINEER can be corrected with program's specific methods, or adding new surfaces compatible with the surface's measured geometry. It is obtained a solid 3D body with specific characteristics which depends by the material; with its help, numeric simulations of forces at impact can be done. After ingeneration the 3D cast, the action of mastication forces over the solid, are necessary for describing the stages:

1. solid 3D geometric shape created by PROENGINEER;
2. solid takes the materials characteristics. The program will calculate the volume taken by the cast and it's weight depending by the material (values used can be found in "anexa 1");
3. compromising 3D cast;
4. assert temperature conditions if it is necessary. In this case the program consider a temperature of 22⁰C, when no reactions of the solid cast took place;
5. assert attests to solid cast. This attest can be external loadings, solid fixation, (conditions assert at the limit of the cast's position in a manner that external loads over the cast are not producing any modifications) etc. The program calculates the cast's answer at the attests.
6. answer to numeric simulation. Program select it's own method of solving the problem. It will be selected from a list what can be determined, the once that represent attention for the studied cast.

The 3D solid body was obtained from a CAD ProEngineer graphic file. The considered size was 29,92mm on OX ax, 11,35mm on OY ax and 7,26mm on OZ ax. The compromise of 3D body is presented by 81451 bows and 53649 elements. The mastication forces generated a medium magnitude of 200N for vertical component of external loads of partial fix denture. The action of this force was distributed in 5 points.. The targeted areas for the PSOCT investigations were especially those of maxim tensions revealed by the numerical simulations.

IV. PSOCT RESULTS

PSOCT images from different metal-ceramic fixed partial prostheses are shown below. Using incisal scanning we found many pores which can cause possible fractures of the investigated dental bridges due to its dimensions and its positions. All the pores depicted below are deep in the dental ceramic material; therefore it will be hard to be detected via normal visual inspection. The material defects within the ceramic layers for metal-ceramic prostheses. The detected defects have a large volume highly capable to generate fracture lines in the proximal or almost superficial on the occlusal area, leading to the failure of the prosthetic treatment. The detection of these defects before inserting the prostheses allows all the corrections in order to avoid the fracture of the ceramic component. For a better understanding of the ceramic defect spreading a three dimensional reconstruction can be develop.

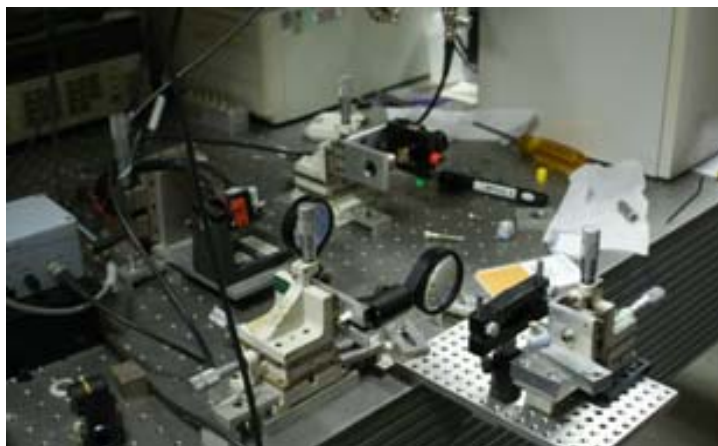


Fig.5. A part of the PS-OCT system architecture.

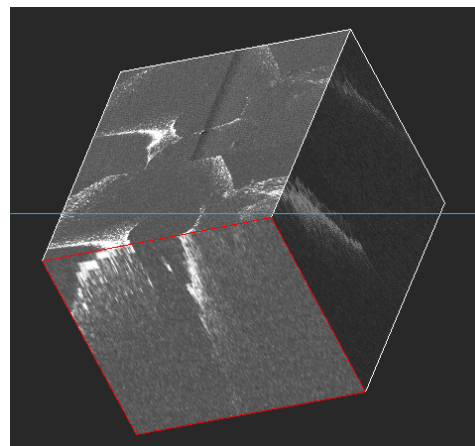
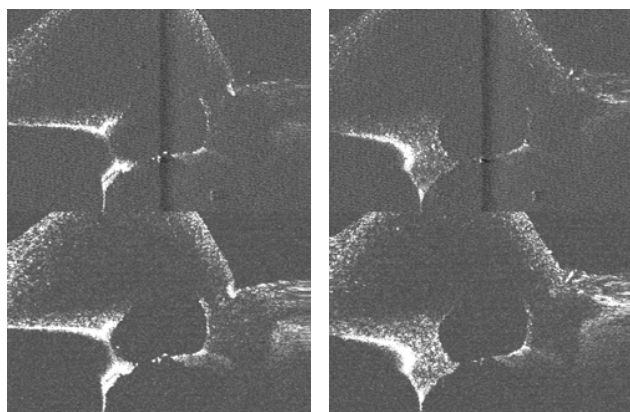


Fig. 8. Detail of the ceramic defect in the 3D reconstruction for sample 29. Note the magnitude of the defect inside the ceramic layers.



a

b

Fig. 6. Metal Ceramic Fixed Partial Denture Sample 29 investigated with PS-OCT: a. slice 28 from 118 and b. slice 37 from 118. Notice the big ceramic defect in the centre of the image.

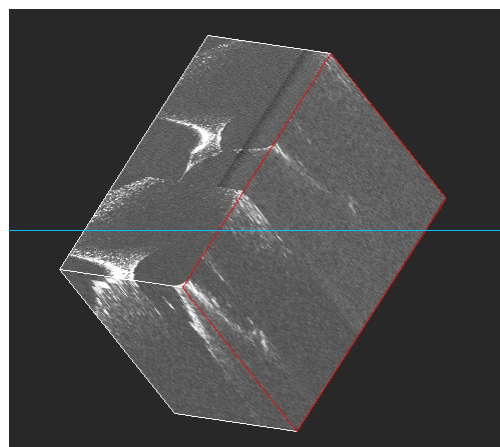


Fig.9. Detail of the ceramic defect in the 3D reconstruction for sample 29. Note the magnitude of the defect inside the ceramic layers.

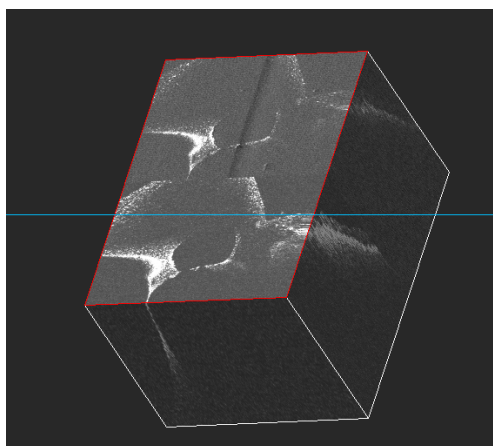


Fig.7. 3D reconstruction of the ceramic defect situated in depth of the metal ceramic fixed partial denture sample nr. 29.



Fig. 10. The material defect inside the ceramic layers after the detection in the sample 29.

V. NUMERICAL SIMULATION RESULTS

The numerical simulation was performed in FEM using COSMOS/M software package (Fig. 9). For the investigation only the tooth (molar 3.6) with the depicted ceramic defect was considered. In order to simplify the numerical analysis, considering the mesio-distal strain on this tooth are zero (because of the presence of the premolar 3.5. and molar 3.7. from the fixed partial dentures), the numerical simulation become a plane strain problem. The location of the defect was considered to be in positions in ceramic depth ($d/d_{max} = 0.5294$), between the occlusal surface and the metallic infrastructure. The material properties of the considered materials were taken from the material library of the software: $E = 2.21e5$ MPa (Young's modulus) and $\nu = 0.22$ (Poisson's Ratio) for the ceramic material and $E = 2.1e5$ MPa (Young's modulus) and $\nu = 0.31$ (Poisson's Ratio) for the metallic infrastructure.

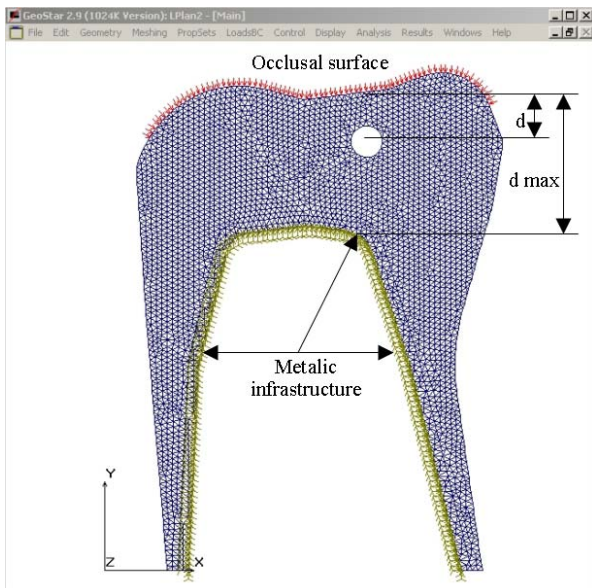


Fig. 9. The numerical simulation for the sample considered: meshing the structure with the defect and boundary conditions.

The boundary conditions were imposed as fixed on the inner part of the metallic infrastructure and the pressure normal on the occlusal surface, constant in value ($p = 1$ MPa) on the strict occlusal area and linear on the two occluso-proximal areas (the pressure decrease from 1 MPa to zero).

The maximum tensile stresses occurred on the vertical diameter of the defect could initiate fracture lines towards occlusal surface and/or metal infrastructure. Starting from these points a simulation of crack initiation and propagation was carried out for two cases: when the crack initiates on the upper point and grows toward occlusal surface (Fig. 12), and crack initiates on the lower point and propagates towards the metal infrastructure (Fig. 13). The crack propagation simulation was performed according with the maximum tensile stress criteria of Sih and Erdogan [13], and a remesh and fill algorithms was used to extend the crack [14]. A 0.05 mm crack increment was considered. The stress intensity

factors were calculated based on displacement correlation method.

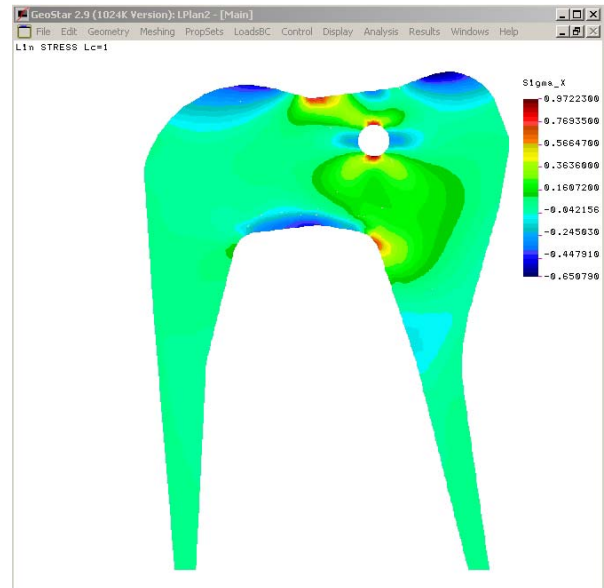


Fig.10. The numerical simulation for the sample considered: results of the stress analysis on ox axe.

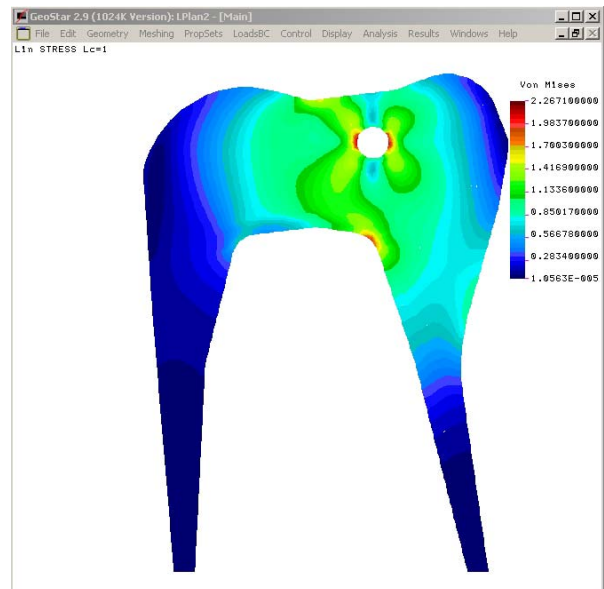


Fig. 11. The numerical simulation for the sample considered: results of the stress analysis on ox and oy axes.

VI. DISCUSSION

There are several factors that are associated with the stress state created in ceramic restorations, including: thickness of ceramic layers, mechanical properties of the materials, elastic modulus of the supporting substrate material, direction, magnitude and frequency of applied load, size and location of occlusal contact areas, residual stresses induced by processing or pores, restoration-cement interfacial defects and environmental defects. This study is focused on fractures

causes by residual stress induced by included pore facing masticatory forces. The PSOCT technique from this study allows a complex characterization process. First, it was possible to detect the pores inside the metal – ceramic fixed partial dentures. The detected defects have a large volume highly capable to generate fracture lines in the proximal or almost superficial on the occlusal area, leading to the failure of the prosthetic treatment. The detection of these defects before inserting the prostheses allows all the corrections in order to avoid the fracture of the ceramic component. The simulation of crack propagation shows that the crack could initiate from the upper or lower limits of defect and propagates through the ceramic material where a tensile stress field is present. This is a major factor in failure of metal ceramic fixed partial dentures.

VII. CONCLUSION

The detection of ceramic defects before oral inserting the prostheses allows all the corrections in order to avoid the fracture of the ceramic component. The fractures that occur within the structure of these prostheses were motivated by the elasticity module of the ceramics and by the defects within the ceramic layers. Early detection of substance defects within these layers allows for optimal corrections before inserting them and applying masticatory stress together with reduction of fractures. Also some of the defects are situated superficial enough and cervical, namely in the maximum tension area recorded during mastication with high risks of fracture at this level.

REFERENCES

- [1] Bratu D., R. Nussbaum – *Bazele clinice și tehnice ale protezării fixe*, Editura Signata, 2001.
- [2] Cosmin Sinescu, Meda Negruțiu, Carmen Todea, Adrian Gh. Podoleanu, Mike Huighes, Philippe Laissue, Cezar Clonda - *Optical Coherecte Tomography as a non invasive method used in ceramic material defects identification in fixed partial dentures*, Dental Target, nr. 5, year II, 2007.
- [3] A. Gh. Podoleanu, J. A. Rogers, D. A. Jackson, S. Dunne, *Three dimensional OCT images from retina and skin* Opt. Express, Vol. 7, No. 9, p. 292-298, (2000), <http://www.opticsexpress.org/framestocv7n9.htm>.
- [4] B. R. Masters, *Three-dimensional confocal microscopy of the human optic nerve in vivo*, Opt. Express, 3, 356-359 (1998), <http://epubs.osa.org/oearchive/source/6295.htm>.
- [5] J. A. Izatt, M. R. Hee, G. M. Owen, E. A. Swanson, and J. G. Fujimoto, *Optical coherence microscopy in scattering media*, Opt. Lett. 19, 590-593 (1994).
- [6] C. C. Rosa, J. Rogers, and A. G. Podoleanu, *Fast scanning transmissive delay line for optical coherence tomography*, Opt. Lett. 30, 3263-3265 (2005).
- [7] A. Gh.P odoleanu, G. M. Dobre, D. J. Webb, D. A. Jackson, *Coherence imaging by use of a Newton rings sampling function*, Optics Letters, 21(21), 1789, 1996.
- [8] A. Gh. Podoleanu, M. Seeger, G. M. Dobre, D. J. Webb, D. A. Jackson and F. Fitzke, *Transversal and longitudinal images from the retina of the living eye using low coherence reflectometry*, Journal of Biomedical Optics, 3, 12, 1998
- [9] Cosmin Sinescu, Adrian Podoleanu, Meda Negruțiu, Mihai Romînu – *Optical coherent tomography investigation on apical region of dental roots*, European Cells & Materials Journal, Vol. 13, Suppl. 3, 2007, p.14, ISSN 1473-2262.
- [10] C Sinescu, A Podoleanu, M Negrutiu, C Todea, D Dodenciu, M Rominu, *Material defects investigation in fixed partial dentures using optical coherence tomography method*, European Cells and Materials Vol. 14. Suppl. 3, ISSN 1473-2262, 2007.
- [11] Roxana Romînu, C Sinescu, A Podoleanu, M Negrutiu, M Romînu, A Soicu, C Sinescu, *The quality of bracket bonding studied by means of oct investigation. A preliminary study*, European Cells and Materials Vol. 14. Suppl. 3, ISSN 1473-2262, 2007.
- [12] Cosmin Sinescu, Meda Lavinia Negrutiu, Carmen Todea, Cosmin Balabuc, Laura Filip, and Roxana Romînu, Adrian Bradu, Michael Hughes, and Adrian Gh. Podoleanu, *Quality assessment of dental treatments using en-face optical coherence tomography*, J. Biomed. Opt., Vol. 13, 054065 (2008).
- [13] F. Erdogan, G.C. Sih : *On the crack extension in plates under plane loading and transverse shear*, J Basic Engineering vol. 85, 4, (1963).
- [14] Wawrzynek P.A., Ingraffea A. R.: *Discrete modeling of crack propagation: theoretical aspects and implementation issues in two and three dimensions*. Cornell University, Ithaca, NY, (1991).

Open Science Index, Biomedical and Biological Engineering Vol:3, No:5, 2009 publications.waset.org/12206.pdf

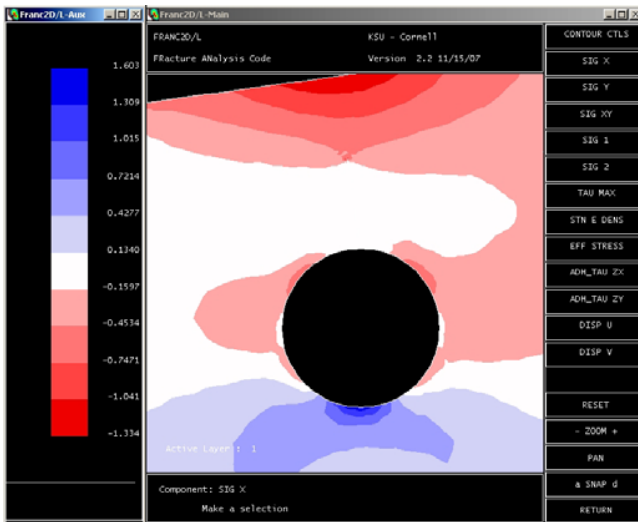


Fig. 12. The crack propagation towards the occlusal surface: the stress field around crack.

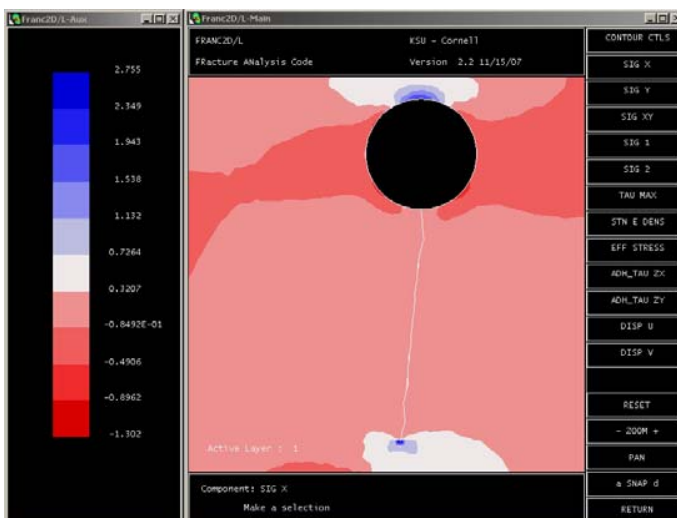


Fig. 13. The crack propagation towards the metal infrastructure: the stress field around crack.